Travelling-wave spatially periodic forcing of asymmetric binary mixtures

Lennon Ó Náraigh

School of Mathematics and Statistics, University College Dublin, Belfield, Dublin 4, Ireland

19th November 2018

Context of work I

- Below a critical temperature, mixtures made up of two immiscible components may separate into their component parts.
- This happens in applications including polymer science and metallurgy.

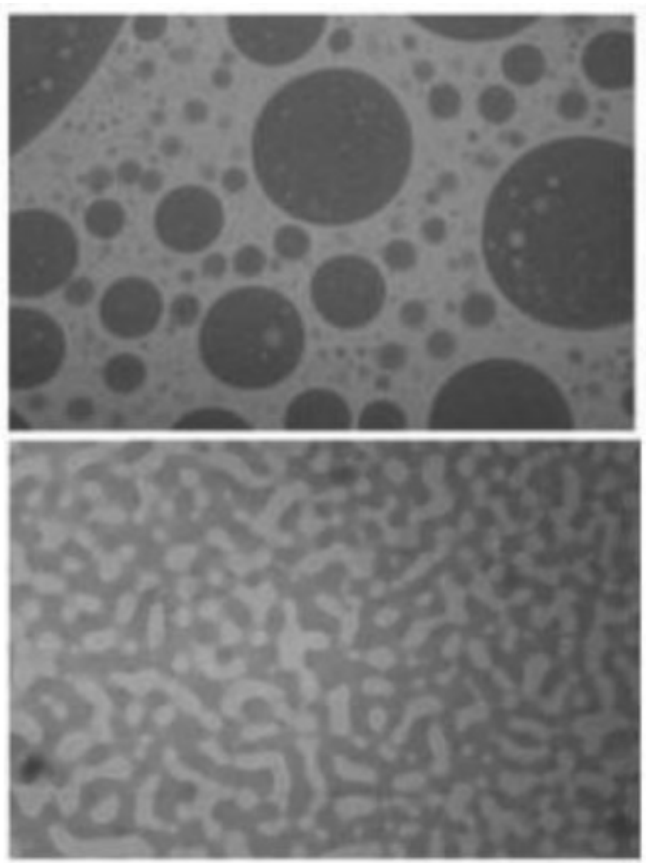

(a) Phase separation in a polymer mixture

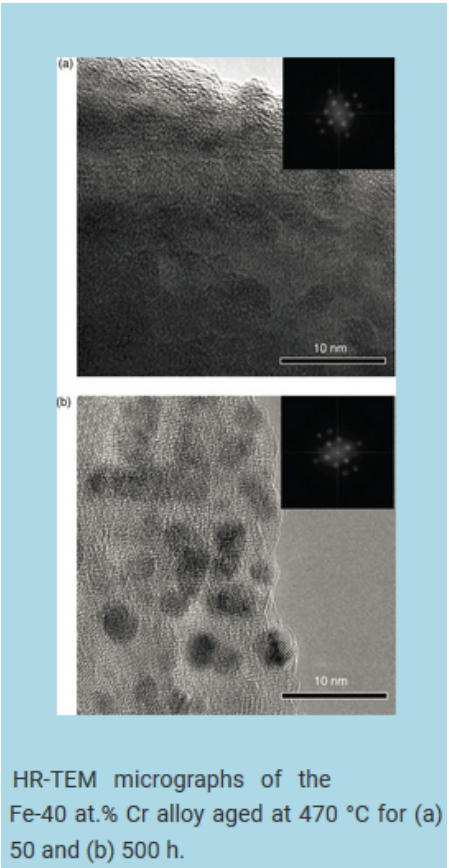

(b) Phase separation in a molten alloy

Context of work II

A mathematical model (first introduced for the binary alloys) for phase separation is the Cahn–Hilliard equation:

$$\frac{\partial c}{\partial t} = D\nabla^2\left(c^3 - c - \gamma\nabla^2 c\right), \qquad \text{[Note: } \frac{\mathrm{d}}{\mathrm{d}t}\int_\Omega c(\boldsymbol{x},t)\mathrm{d}^n x = 0\text{]},$$

where c is the concentration field, D is the diffusion coefficient and $\sqrt{\gamma}$ is a length.

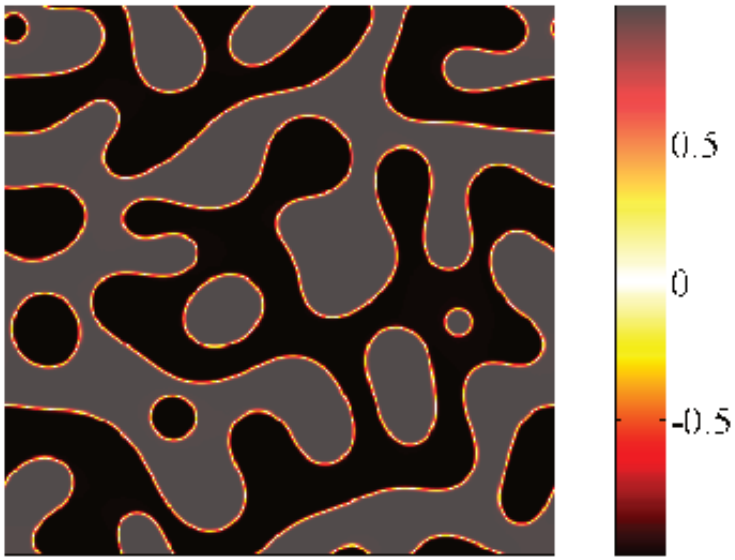

The solution is $c = \pm 1$ in domains with transition regions of thickness $\sqrt{\gamma}$ in between. The domains grow in time. The constant solution $c = 0$ is a well-mixed state but it is unstable.

The values $c = \pm 1$ are energetically favourable.

Context of work III

- In applications, it can be desirable to 'tune' the phase separation to achieve a certain outcome – for instance, a certain well-defined structure for the domains.
- In this talk we look at **travelling-wave forcing** as a means of achieving this – this can be achieved in practice by differential heating of the binary fluid and hence, inducing concentration gradients via temperature gradients.

Context of work III

- In applications, it can be desirable to 'tune' the phase separation to achieve a certain outcome – for instance, a certain well-defined structure for the domains.
- In this talk we look at **travelling-wave forcing** as a means of achieving this – this can be achieved in practice by differential heating of the binary fluid and hence, inducing concentration gradients via temperature gradients.
- The focus of this talk is on developing an analytical theory – we therefore look at a simple model with a travelling-wave **forcing term** in one spatial dimension:

$$\frac{\partial c}{\partial t} = D\frac{\partial^2}{\partial x^2}\left(c^3 - c - \gamma\frac{\partial^2 c}{\partial x^2}\right) + f_0 k\cos[k(x-vt)], \qquad x \in (-\infty, \infty),$$

where f_0 is the forcing amplitude, etc.

Context of work III

- In applications, it can be desirable to 'tune' the phase separation to achieve a certain outcome – for instance, a certain well-defined structure for the domains.
- In this talk we look at **travelling-wave forcing** as a means of achieving this – this can be achieved in practice by differential heating of the binary fluid and hence, inducing concentration gradients via temperature gradients.
- The focus of this talk is on developing an analytical theory – we therefore look at a simple model with a travelling-wave **forcing term** in one spatial dimension:

$$\frac{\partial c}{\partial t} = D\frac{\partial^2}{\partial x^2}\left(c^3 - c - \gamma\frac{\partial^2 c}{\partial x^2}\right) + f_0 k\cos[k(x-vt)], \qquad x \in (-\infty, \infty),$$

  where f_0 is the forcing amplitude, etc.
- With appropriate boundary conditions, the forcing term is consistent with the conservation of the spatial mean concentration,

$$\frac{\mathrm{d}}{\mathrm{d}t}\int_{-\infty}^{\infty} c(x,t)\,\mathrm{d}x = 0.$$

Preliminaries I

- We seek travelling-wave **periodic** solutions of the forced Cahn–Hilliard equaiton,

$$c(x,t) = \psi(\eta), \qquad \eta = x - vt, \qquad \psi(\eta + L) = \psi(\eta), \qquad L = 2\pi/k.$$

- As such, we seek solutions of the ODE

$$-\frac{\mathrm{d}\psi}{\mathrm{d}\eta} = D\frac{\mathrm{d}^2}{\mathrm{d}\eta^2}\left(\psi^3 - \psi - \gamma\frac{\mathrm{d}^2\psi}{\mathrm{d}\eta^2}\right) + f_0 k\cos(k\eta).$$

- We can integrate once to reduce the order. After eliminating constants of integration, we get

$$\gamma D\frac{\mathrm{d}^3\psi}{\mathrm{d}\eta^3} = D\frac{\mathrm{d}}{\mathrm{d}\psi}(\psi^3 - \psi) + v(\psi - \langle\psi\rangle) + f_0\sin(k\eta), \tag{1}$$

Spatial average: $\langle\psi\rangle = L^{-1}\int_0^L \psi(\eta)\,\mathrm{d}\eta$.

The aim of the talk is to characterize the solutions of Equation (1).

Preliminaries II

Motivated by applications, we can take $\epsilon = \gamma/L^2 \to 0$. We attempt a regular perturbation theory, with $\psi(\eta) = \psi_0(\eta) + \epsilon\psi_1(\eta) + \cdots$. This quickly gives us two important scenarios:

Preliminaries II

Motivated by applications, we can take $\epsilon = \gamma/L^2 \to 0$. We attempt a regular perturbation theory, with $\psi(\eta) = \psi_0(\eta) + \epsilon\psi_1(\eta) + \cdots$. This quickly gives us two important scenarios:

1. **The regular limit:** The regular perturbation theory is valid, and we solve

$$0 = D\frac{\mathrm{d}}{\mathrm{d}\psi}(\psi^3 - \psi) + v(\psi - \langle\psi\rangle) + f_0 \sin(k\eta),$$

   i.e. a first-order inhomogeneous ODE (**reduced-order model**).
2. **The singular limit** applies when the regular perturbation theory breaks down. The singular limit requires an examination of the ODE (1) with higher derivatives (**the full model**).

Preliminaries II

Motivated by applications, we can take $\epsilon = \gamma/L^2 \to 0$. We attempt a regular perturbation theory, with $\psi(\eta) = \psi_0(\eta) + \epsilon\psi_1(\eta) + \cdots$. This quickly gives us two important scenarios:

1. **The regular limit:** The regular perturbation theory is valid, and we solve

$$0 = D\frac{\mathrm{d}}{\mathrm{d}\psi}(\psi^3 - \psi) + v(\psi - \langle\psi\rangle) + f_0 \sin(k\eta),$$

   i.e. a first-order inhomogeneous ODE (**reduced-order model**).
2. **The singular limit** applies when the regular perturbation theory breaks down. The singular limit requires an examination of the ODE (1) with higher derivatives (**the full model**).

Important solution: When $f_0 = v = 0$, we have the following special solution of the full model:

$$\psi(\eta) = \tanh\left(\frac{\eta - \eta_0}{\sqrt{\gamma}}\right).$$

Knowing this will later on help us to characterize the singular limit (full model) with f_0 and v nonzero, but with $\epsilon \to 0$.

Reduced-order model – parameter space

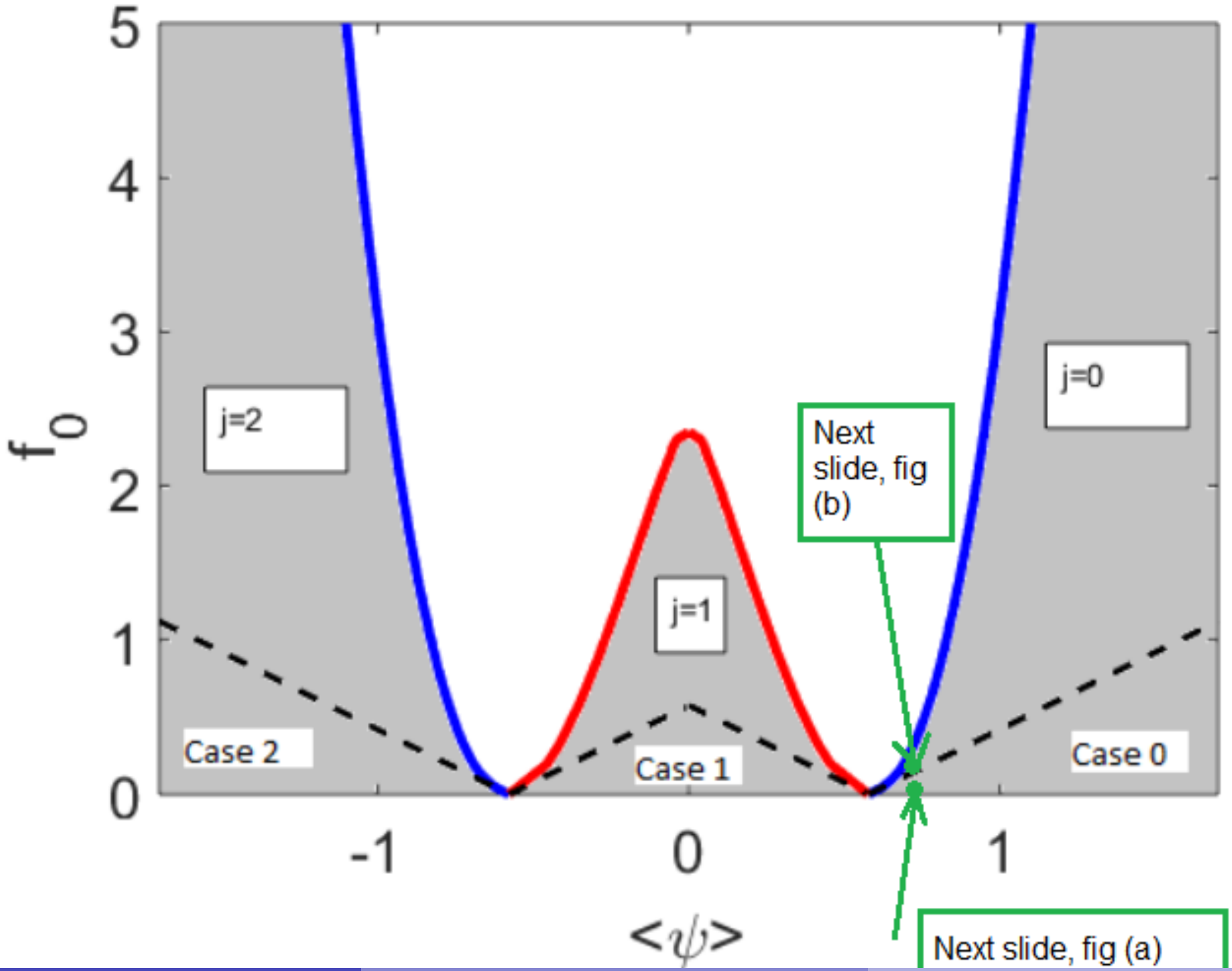

The white area in the parameter space indicates a breakdown of the reduced-order model

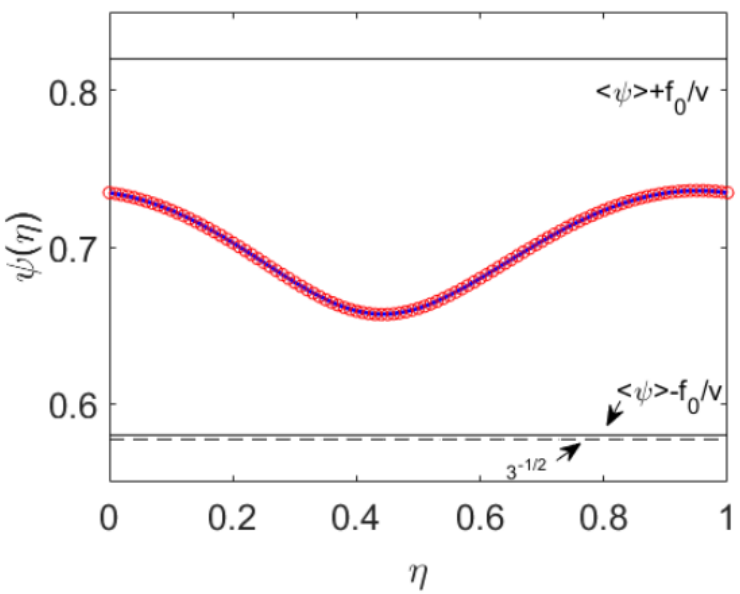

(a) $f_0 = 0.12$

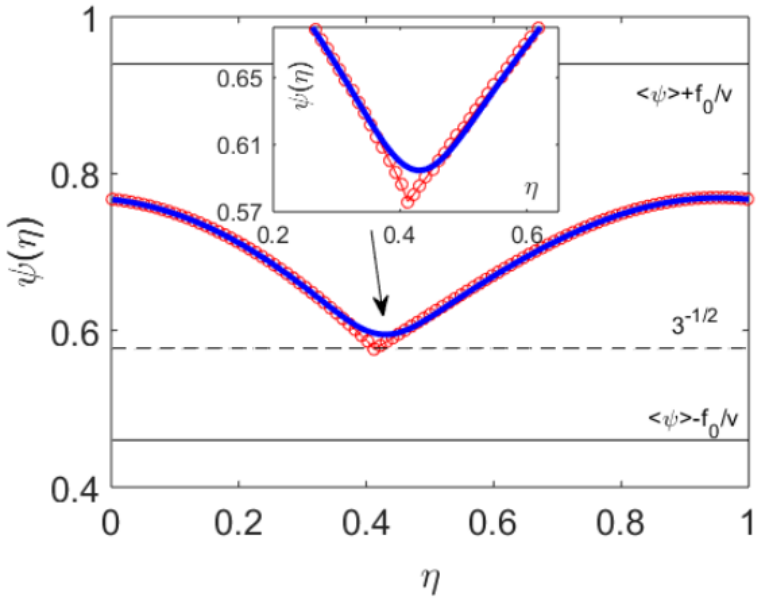

(b) $f_0 = 0.24$

Sample L-periodic numerical solutions of the full model (Equation (5), solid line, with $\epsilon = 10^{-4}$) and the reduced-order model (Equation (7), circles). The following parameters are the same in both panels: $\langle\psi\rangle = 0.7$, $v = D = L = 1$, $k = 2\pi$. The inset in panel (b) is an enlargement of the main figure which shows the formation of the cusp in more detail. Details of the numerical method are provided below at the foot of this section (Section II) and also in A.

Reduced-order model – Rigorous theoretical analysis

- Although the figure explains everything, it is not rigorous.

Reduced-order model – Rigorous theoretical analysis

- Although the figure explains everything, it is not rigorous.
- We can prove rigorous results in the subcases, e.g. **Case 1**, with initial conditions in the range

$$I = [a, b] = [\langle \psi \rangle - (f_0/v), \langle \psi \rangle + (f_0/v)].$$

Reduced-order model – Rigorous theoretical analysis

- Although the figure explains everything, it is not rigorous.
- We can prove rigorous results in the subcases, e.g. **Case 1**, with initial conditions in the range

$$I = [a, b] = [\langle\psi\rangle - (f_0/v), \langle\psi\rangle + (f_0/v)].$$

- We construct a map $f : I \to \mathbb{R}$ that takes initial conditions ($\eta = 0$) in I to final conditions at $\eta = L$. Only delicately-chosen initial/final conditions lead to periodic solutions.

Reduced-order model – Rigorous theoretical analysis

- Although the figure explains everything, it is not rigorous.
- We can prove rigorous results in the subcases, e.g. **Case 1**, with initial conditions in the range

$$I = [a, b] = [\langle\psi\rangle - (f_0/v), \langle\psi\rangle + (f_0/v)].$$

- We construct a map $f : I \to \mathbb{R}$ that takes initial conditions ($\eta = 0$) in I to final conditions at $\eta = L$. Only delicately-chosen initial/final conditions lead to periodic solutions.
- Periodic solutions of the reduced-order model correspond to fixed points of the map, i.e. $f(\psi_*) = \psi_*$ corresponds to a periodic solution $\psi(\eta + L) = \psi(\eta)$, with $\psi(0) = \psi(L) = \psi_*$.

Reduced-order model – Rigorous theoretical analysis

- Although the figure explains everything, it is not rigorous.
- We can prove rigorous results in the subcases, e.g. **Case 1**, with initial conditions in the range

$$I = [a, b] = [\langle\psi\rangle - (f_0/v), \langle\psi\rangle + (f_0/v)].$$

- We construct a map $f : I \to \mathbb{R}$ that takes initial conditions ($\eta = 0$) in I to final conditions at $\eta = L$. Only delicately-chosen initial/final conditions lead to periodic solutions.
- Periodic solutions of the reduced-order model correspond to fixed points of the map, i.e. $f(\psi_*) = \psi_*$ corresponds to a periodic solution $\psi(\eta + L) = \psi(\eta)$, with $\psi(0) = \psi(L) = \psi_*$.
- We have used **Brouwer's Fixed Point Theorem** to show that this map exists for the subcases 0-2. We have used **Banach's Fixed Point Theorem** to show uniqueness.

The full model

- We look now at the full model – this covers cases where the reduced-order model breaks down.

The full model

- We look now at the full model – this covers cases where the reduced-order model breaks down.
- The full model is recalled here as (nondimensional, with $\gamma \to \epsilon$ and $D \to 1$) corresponding to the small interface width:

$$\epsilon \frac{\mathrm{d}^3\psi}{\mathrm{d}\eta^3} = \frac{\mathrm{d}}{\mathrm{d}\eta}\left(\psi^3 - \psi\right) + v\left(\psi - \langle\psi\rangle\right) + f_0 \sin(k\eta). \tag{2}$$

The full model

- We look now at the full model – this covers cases where the reduced-order model breaks down.
- The full model is recalled here as (nondimensional, with $\gamma \to \epsilon$ and $D \to 1$) corresponding to the small interface width:

$$\epsilon \frac{\mathrm{d}^3\psi}{\mathrm{d}\eta^3} = \frac{\mathrm{d}}{\mathrm{d}\eta}\left(\psi^3 - \psi\right) + v\left(\psi - \langle\psi\rangle\right) + f_0 \sin(k\eta). \tag{2}$$

- A first approach is to do direct numerical simulations of the corresponding temporally-evolving equation (TENS):

$$\frac{\partial c}{\partial t} - v\frac{\partial c}{\partial \eta} = \frac{\partial^2}{\partial \eta^2}\left(c^3 - c - \epsilon\frac{\partial^2 c}{\partial \eta^2}\right) + f_0 k \cos(k\eta), \text{ (moving frame).} \tag{3}$$

The full model

- We look now at the full model – this covers cases where the reduced-order model breaks down.
- The full model is recalled here as (nondimensional, with $\gamma \to \epsilon$ and $D \to 1$) corresponding to the small interface width:

$$\epsilon \frac{\mathrm{d}^3\psi}{\mathrm{d}\eta^3} = \frac{\mathrm{d}}{\mathrm{d}\eta}\left(\psi^3 - \psi\right) + v\left(\psi - \langle\psi\rangle\right) + f_0 \sin(k\eta). \tag{2}$$

- A first approach is to do direct numerical simulations of the corresponding temporally-evolving equation (TENS):

$$\frac{\partial c}{\partial t} - v\frac{\partial c}{\partial \eta} = \frac{\partial^2}{\partial \eta^2}\left(c^3 - c - \epsilon\frac{\partial^2 c}{\partial \eta^2}\right) + f_0 k \cos(k\eta), \text{ (moving frame).} \tag{3}$$

- From the TENS (Equation (3)) we look for the emergence of travelling-wave solutions $c(\eta, t) \to \psi(\eta)$ – i.e. solutions of (2).

Two distinct travellling-wave solutions are observed in the full model

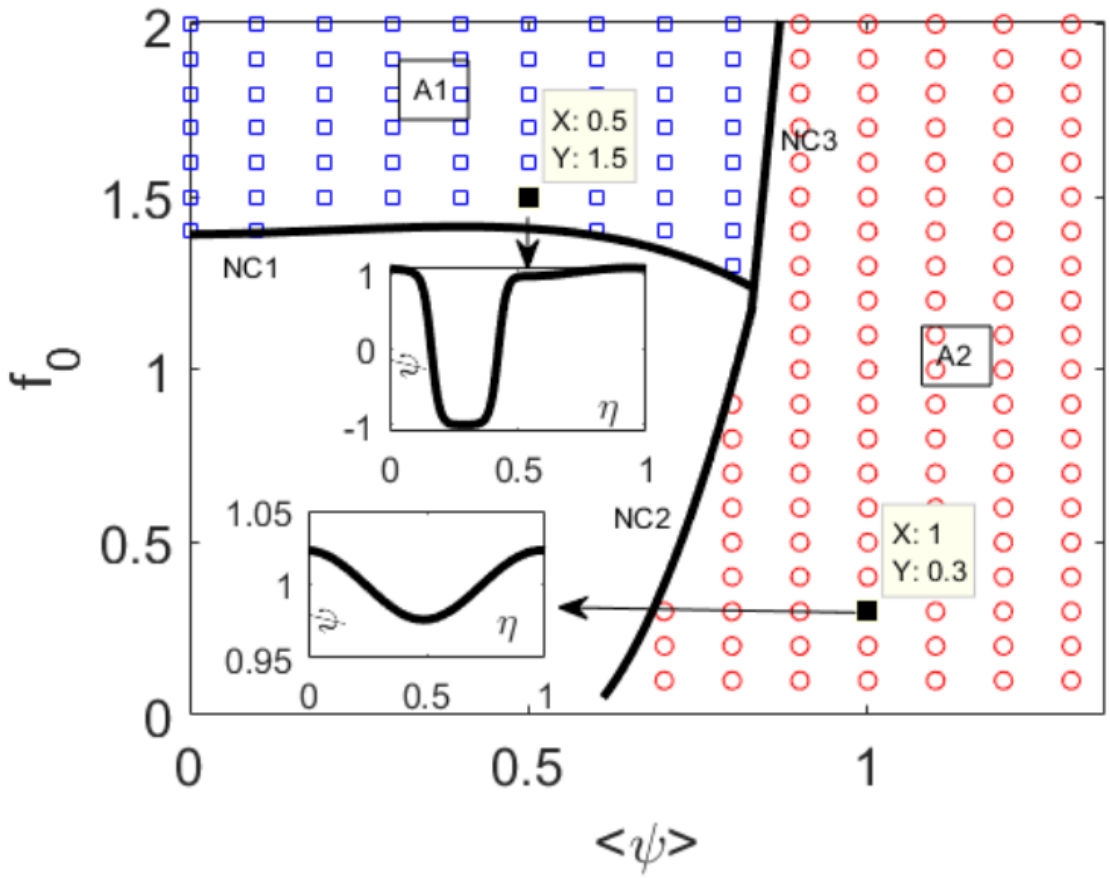

Summary of results of temporally-evolving numerical simulations for fixed $v = 1$, and for various values of $\langle\psi\rangle$ and f_0. Also, the small parameter ϵ is set to 5×10^{-4}. The circles and squares indicate simulations where a steady travelling wave exists.

A1 travelling waves

- The A1 travelling waves (blue squares) are new. These can be understood using an intuitive singular perturbation theory, valid as $\epsilon \to 0$.
- This theory dates back to ideas by Ockendon, Cox, and Mackey, who used the same approach for forced waves in shallow-water models.
- Details are skipped – inner solution is tanh-like profiles; outer solution is a balance between cubic and forcing terms – these are matched by hand in an informal version of the theory.
- Theory valid only for $v = 0$; travelling-wave velocity interpreted as a phase shift.

The Newton solver

The idea now is to use this informal theory to construct approximate solution as a **starting value** in a **Newton solver** for Equation (2). This works!

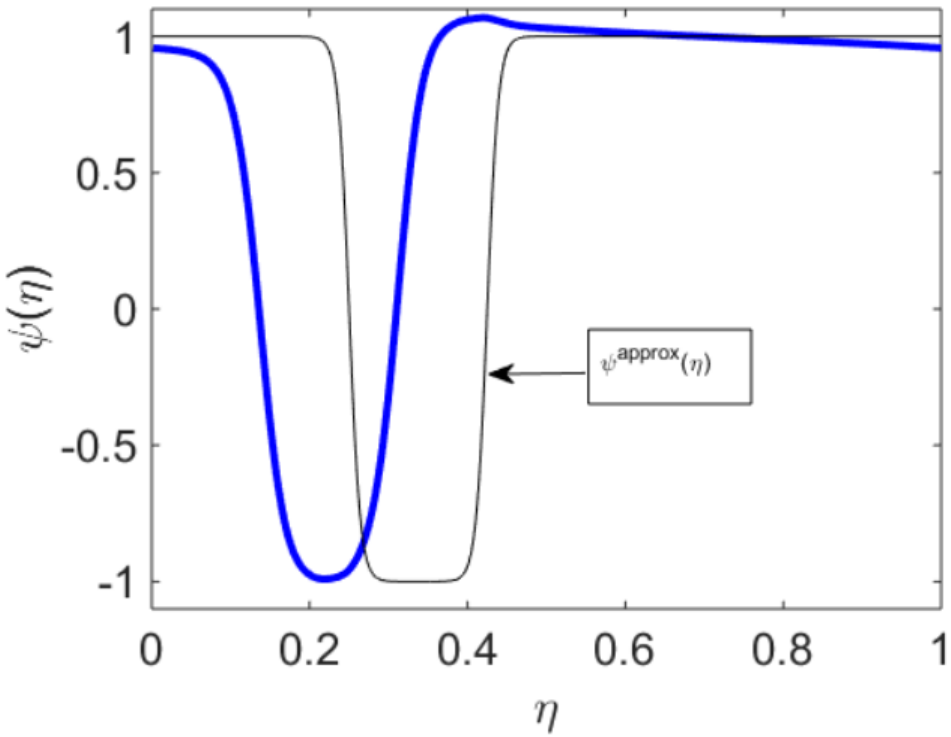

Emergence of single-spike concentration profile from the inital guess $\psi^{\text{approx}}(\eta)$ given by Equation (41). Parameters: $\langle\psi\rangle = 0.65$, $f_0 = 0.1$.

Conclusions

- We have rigorously analyzed the travelling-wave solutions of the forced Cahn–Hilliard equation.
- The analysis relies on a range of tools from Dynamical Systems.
- Construction of a variety of travelling-wave solutions has been accomplished with a Newton solver with a judiciously-chosen initial guess.
- The analysis reveals that the mean concentration $\langle \psi \rangle$ and the forcing amplitude f_0 are key parameters that control the shape of the travelling-wave solutions.
- Submitted work:

  https://arxiv.org/abs/1807.08538

- Thanks to Ted Cox for showing me this problem.

Solutions constructed using the Newton Solver agree with the TENS

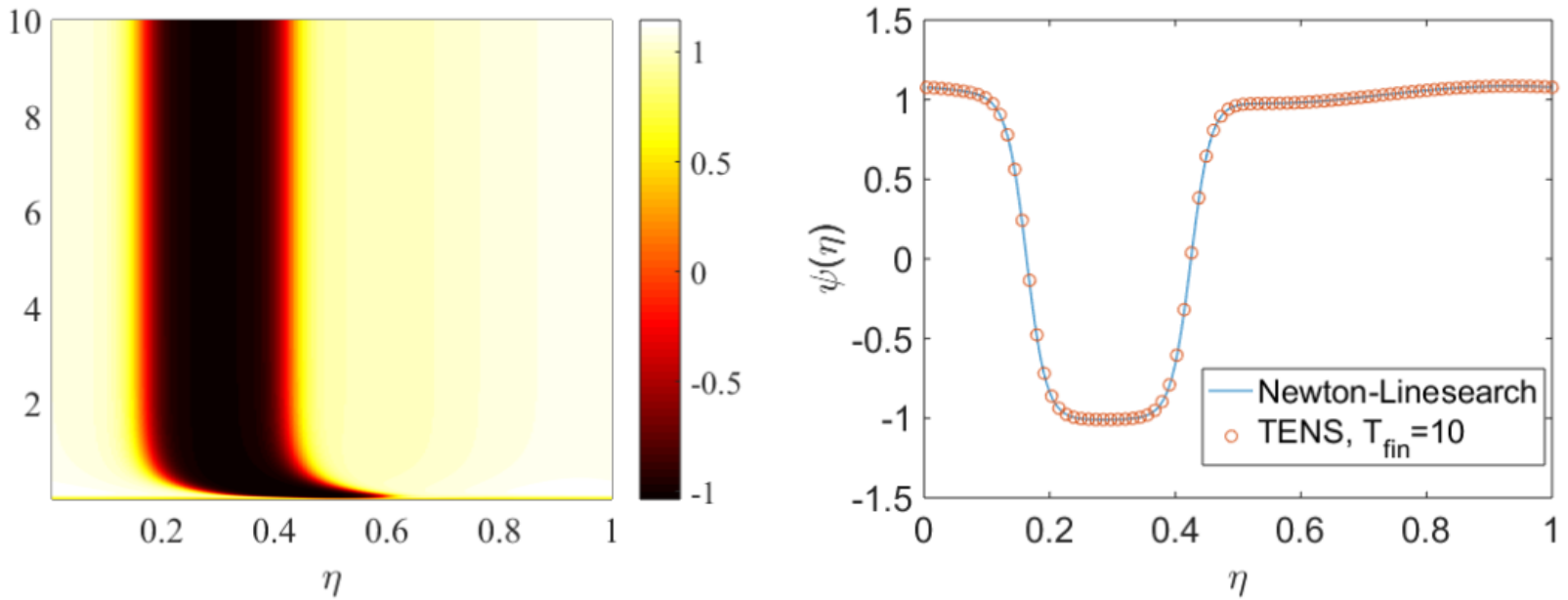

Sample transiently-evolving numerical simulation (TENS) results for the case $\langle\psi\rangle = 0.5$ and $f_0 = 1.5$. Also, $v = 1$, and $\epsilon = 5 \times 10^{-4}$. Panel (a) shows the spacetime evolution of the concentration profile $C(\eta, t)$, up to a final time $T_{\text{fin}} = 10$. Panel (b) shows a snapshot of the concentration at the final time, and a comparison with a steady travelling-wave profile generated with the Newton solver. A timestep $\Delta t = 10^{-4}$ is used. Also, $N = 256$ gridpoints are used in both numerical methods.

The Newton Solver also produces multiple-spike solutions.

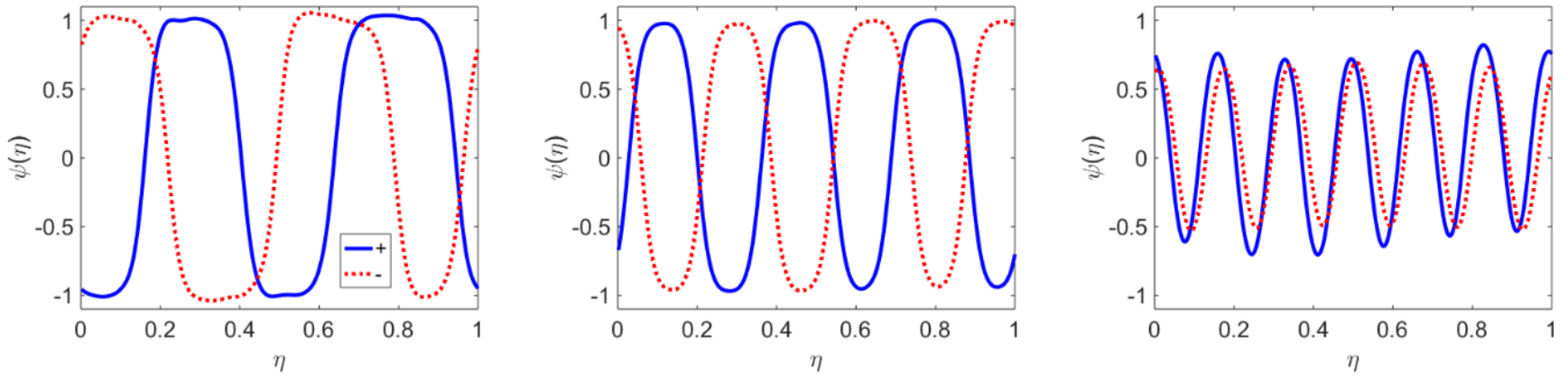

(a) $N = 2$ (b) $N = 3$ (c) $N = 6$

Multiple-spike solutions for $(f_0, v) = (0.1, 1)$ and $\langle\psi\rangle = 0.1$, corresponding to a region in parameter space with no stable travelling waves.

- The theory of initial guesses can also be used to generate multiple-spike solutions.
- These are all linearly unstable, so will only feature transiently in the TENS.
- Cox and Mackey also observed multiple-spike solutions in their work on forced waves in shallow-water models.

Acknowledgments

This project has received funding from the European Union's Horizon 2020 Research and Innovation Programme under grant agreement No 778104

THERMASMART
Thermal Management of Microprocessors